Hot-rolled Zn22Al2Cu-NaCl composite with initial fine-grained and cast-metal matrix microstructures

J. A. Aragon-Lezama

Área de Metalurgia Física y Ciencia e Ingeniería de Materiales, Departamento de Materiales, Universidad Autónoma Metropolitana-A, Av. San Pablo 420, Col. Nueva el Rosario, 02128, Alcaldía Azcapotzalco, CDMX, México.
e-mail: alja@azc.uam.mx

G. Torres-Villaseñor

Departamento de Materiales Metálicos y Cerámicos, Instituto de Investigaciones en Materiales - Universidad Nacional Autónoma de México, Apartado Postal 70-360, México, CDMX, México,
e-mail: gtorres@unam.mx

Received 20 January 2026; accepted 9 April 2026

A composite of a Zn22Al22Cu matrix and NaCl particles was developed to establish whether this material could be hot-rolled and, if feasible, to determine the structural changes according to the initial matrix microstructure and percent section reduction achieved with this process. The composite was made by melting the alloy, adding the particles, molding, compressing the mixture of metal and particles, and air cooling, with an approximate (mass of particles)/(mass of alloy) ratio equal to 0.6. Plates of the composite with the initial cast-metal matrix microstructure and with a heat-treated initial fine-grained matrix microstructure were hot-rolled in two stages to approximately 80% section reduction at 230°C. Plate samples that were not rolled, plates hot-rolled to approximately 50% section reduction and plates hot-rolled to the maximum percent reduction were mirror-polished, and the matrix and NaCl-particle interfaces were analyzed and imaged with a scanning electron microscope. Vickers microhardness was measured in the matrix and in NaCl particles, and Rockwell hardness F of the nonrolled and hot-rolled composites was determined. The cast-metal matrix microstructure acquired shape texture without recrystallization, while the fine-grained matrix microstructure recrystallized with increasing rolling %. The NaCl particles deformed together with the matrix and hardened, with the hardening speed being greater when the matrix was fine-grained. The composite could be hot-rolled with either microstructure, with the cast-metal matrix microstructure being more favorable. The hot-rolling of this material allows the production of thin cellular sheets to be obtained.

Keywords: Hot-rolling; Zn22Al2Cu-NaCl composite; microstructure characterization; hardness.

DOI: https://doi.org/10.31349/RevMexFis.72.051002

1. Introduction

The alloy of eutectoid composition Zn22Al has been studied extensively. It has been known for a long time that this material is superplastic when it has a fine-grained microstructure of a phase rich in Al (α) and another phase rich in Zn (η) and deforms at a quasistatic deformation rate [1,2] at a temperature close to 0.5 T_f (the melting temperature of the alloy), plastically deforming several hundred percent before fracturing.

This microstructure is achieved, for example, by applying a heat treatment to this alloy, consisting of maintaining it at a temperature above 273°C for approximately 45 hours and subsequent tempering in a water or ice-water bath. This procedure has been used alone or in combination with other techniques to study different aspects of the superplastic behavior of this alloy [3-6].

The Zn22Al alloy has been used as a base alloy for the manufacture of other alloys with different types and amounts of solutes, for example, the solutes Cu [7-10], Si [11], Ti [12] Ag [13], Ce [14] and Fe [15], to investigate superplastic behavior, phase transformations, mechanical and physical properties, and evolution of the microstructure.

In addition, the Zn22Al alloy has been used as the matrix of composites [16-18] and has been converted to a foam alloy [19,20] and composite foam [21,22] to investigate mechanical properties.

Among the various alloys derived from the Zn22Al alloy with certain solutes is the Zn22Al2Cu alloy, which has been interesting to researchers and technologists. This alloy is reported to have higher corrosion resistance than galvanized products, can be hot-rolled [23] and is weldable [24]. A fine microstructure is obtained by performing the aforementioned procedure for the Zn22Al alloy without Cu, and this alloy also has superplastic properties [25]. This alloy has been used as a matrix for composites with structural components of Al_2O_3, hydroxyapatite or graphite [26], ZnO [27], solid glass spheres [28,29], and SiC [30] to investigate the mechanical properties of these composites and has been obtained as a cellular alloy [31,32].

One way to make cellular metals is to use particles as space maintainers or NaCl preforms that can be, for exam-

ple, infiltrated by the alloy in the liquid state [33], and the resulting composite in the solid state is immersed in boiling water for a certain amount of time to dissolve NaCl. This cellular alloy has, similar to all materials of its kind, multiple properties and applications [34]. The same cellular alloy can serve as a vibration damper, a support for catalysis, a heat exchanger, a filter, and a protective wrap for fragile objects, with the advantage of having twice the mechanical strength of aluminum foams.

In a related co-authored work involving the authors of this study, concerning the Zn22Al2Cu-NaCl composite with six different densities, two NaCl grain textures, and matrix microstructures similar to those used in this work, tested under compression at room temperature, it was established that the NaCl particles do not reinforce the matrix; rather, they deform along with it, especially when the composite has the lowest density, a cast matrix microstructure, and smoothed NaCl grains [35].

NaCl is an ionic solid with a face-center cubic crystallographic structure. NaCl monocrystals exhibit a stress-strain curve similar to that of metals with the same crystallographic structure [36]. NaCl polycrystals are brittle at room temperature but ductile at temperatures above 200°C [37].

Therefore, the Zn22Al2Cu-NaCl composite is expected to be successfully formed above 200°C, as the superplastic behavior of the matrix alloy also occurs above 200°C for this purpose, sharp NaCl particles could potentially be used.

This work investigates whether the Zn22Al2Cu-NaCl composite can be hot-rolled using two different initial matrix microstructures: one obtained during material fabrication (cast-metal matrix microstructure) and another obtained by heat treatment (fine-grain matrix microstructure).

If hot rolling is possible, the changes in each initial matrix microstructure will be established as the percentage reduction in the composite's cross-section increases. The production of sheets of this composite is crucial, as they can be easily transformed into very thin cellular sheets for use as filters, heat sinks or composite sheets assembled into a stack within an insertable and replaceable cartridge in a water hydrolysis chamber for green hydrogen production. However, additional tests and measurements must be performed, such as, for example, determining the cell size, electrical conductivity, and corrosion resistance of the sheets that will integrate the cartridge.

2. Experimental procedure

2.1. Preparation of the matrix alloy

The Zn22Al2Cu alloy was produced by conventional casting at 700°C. Zn, Al and Cu ingots were used with purities of 99.99%, 99.27% and 99.999%, respectively. A Velab VE-300 scale with a precision of 10^{-4} g was used to obtain the correct quantities of the elements. A zirconia-lined graphite crucible and a Lindberg 5189A muffle furnace were used for the casting. The density of the alloy was obtained by the Archimedean method, resulting in a value of 5.4 g/cm^3.

2.2. NaCl particles

The NaCl particles used had an irregular shape and an average size of 2.25 ± 0.25 mm. The particles were selected by sifting different-sized particles. The physical properties of the particles were an elastic modulus of approximately 40 GPa, a melting temperature of 816°C, and a density of 2.16 g/cm^3.

2.3. Composite manufacturing

The composite was elaborated by remelting 800 g of the alloy at 700°C and preheating 480 g of NaCl particles, equivalent to 0.6 times the mass of the alloy, at 400°C. This ratio ensures the production of a low-density composite, which will have a greater plastic deformation under compression, as found in another research [35] co-led by the authors of this work. The hot NaCl particles were then submerged in the liquid alloy and pushed in with a piston to retain them while the mixture cooled in air until complete solidification.

The average density of the composite was determined by establishing the average value of the mass/volume ratios of several sections. An average density of 3.0835 g/cm^3 was obtained.

Using the equation of the mixture rule [38] for the composite density, in terms of volume fractions and densities of NaCl and matrix alloy, 2.16 g/cm^3 and 5.4 g/cm^3, respectively, and the experimental value of the composite density, 3.0835 g/cm^3, a volume percentage of NaCl 71.5 is obtained.

The composite obtained was cut into two equal parts, and one part was subjected to a heat treatment as described in section 2.4 to change the initial microstructure of the matrix. Subsequently, the two halves of material were cut into 8 mm-thick sections for hot-rolling.

2.4. Microstructures in the matrix

The initial matrix microstructures were obtained by casting and heat-treatment. The first microstructure was formed by air-cooling during the last stage of the composite manufacturing process; the other microstructure was obtained after the composite with cast metal microstructure was heated and maintained at 350°C for 45 hours and then tempered in acetone at 1°C.

Samples of the casting material with heat-treatment were finely ground and submerged in C_2H_6O at 1% HNO_3 to reveal the microstructure. A JEOL JCM 600 portable scanning electron microscope and a JEOL JSM-7600F field emission electron microscope were used to characterize the microstructures. The compositions of the constituents in each initial matrix microstructure of the samples were determined by energy-dispersive X-ray spectroscopy (EDXS).

The microhardnesses (10 g test charge) of the constituents of each initial matrix microstructure and the embedded NaCl

particles and the Rockwell hardness F of the nonrolled composites were determined using a Micromet 2003 microdurometer and a Misawa Seiki Seisakusho durometer.

All measurements were made on both sides of the 0.8 cm thick plate of the composite with one and the other microstructure, performing approximately a similar number of measurements in regions from one end of the plate to the other to complete, according to the dispersion of the data, between 10 and 15 Vickers microhardness measurements on the matrix; 11, on NaCl grains, and between 10 and 27 Rockwell F hardness measurements.

2.5. Hot-rolling process

The alloy without NaCl grains was not hot rolled because this work was performed and reported by Negrete [23].

Plates approximately 8 mm thick with the cast-metal matrix microstructure and the fine-grained matrix microstructure obtained after heat-treatment were hot-rolled at an angular velocity of 10 revolutions/minute (4 mpm) and a temperature of 230°C using a FENN 5^a mill rolling (with rollers of 5" diameter) until a plate thickness reduction of approximately 80% was achieved: the final thickness of the sheets obtained was approximately 1.6 mm. The temperature and angular velocity were chosen based on what has been reported about the rolling Zn22Al2Cu alloy [23].

The effects of rolling on the composite were evaluated with metallographic studies, making observations and taking images of different zones of the matrix and interfaces between constituents in plates with different microstructures and with approximately 50% and 80% reductions in thickness using the electronic microscopes mentioned in Sec. 2.4.

The average Vickers microhardness of constituents in resulting microstructures and the medium Rockwell hardness F of the hot-rolled plates were determined by taking a similar measurements number on both sides of the sheets, as described in the previous section, after each percentage reduction in area. The compositions of different microstructural zones in the matrix were determined by EDXS. The samples used had been previously polished with a diamond suspension and then subjected to ultrasonic cleaning with acetone and drying with warm air.

3. Results

3.1. Microstructures in the matrix

3.1.1. Initial microstructures

The initial cast-metal matrix microstructure of the nonrolled composite is shown in Fig. 1a). The microstructure consisted of dendrites and an interdendritic component.

The compositions determined by EDXS in the different zones (dendrite center, dendrite edge, interdendritic contour and interdendritic zone) of the initial cast-metal matrix microstructure are presented on the left side of Table I. These data show that the Zn and Cu contents increased and the Al content decreased from the center of the dendrites to the interdendritic zone. The Cu content in the interdendritic contours did not follow this pattern, as the amount of Cu measured in this zone was less than the amount of Cu at the dendrite edge.

TABLE I. Composition of the constituents in the nonrolled initial cast-metal matrix microstructure and 47.6% hot-rolled composite by EDXS.

	Not rolled			47% **hot-rolled**		
Constituent or region	Zn(%p)	Al(%p)	Cu(%p)	Zn(%p)	Al(%p)	Cu(%p)
Dendritic center	52.70	46.29	0.40	61.07	38.93	0.00
Dendrite edge	63.42	34.04	2.54	71.59	28.41	0.00
Interdendritic contour	67.97	30.72	1.31	89.00	3.96	7.05
Interdendritic zone	93.14	2.22	4.64	91.36	2.51	6.13

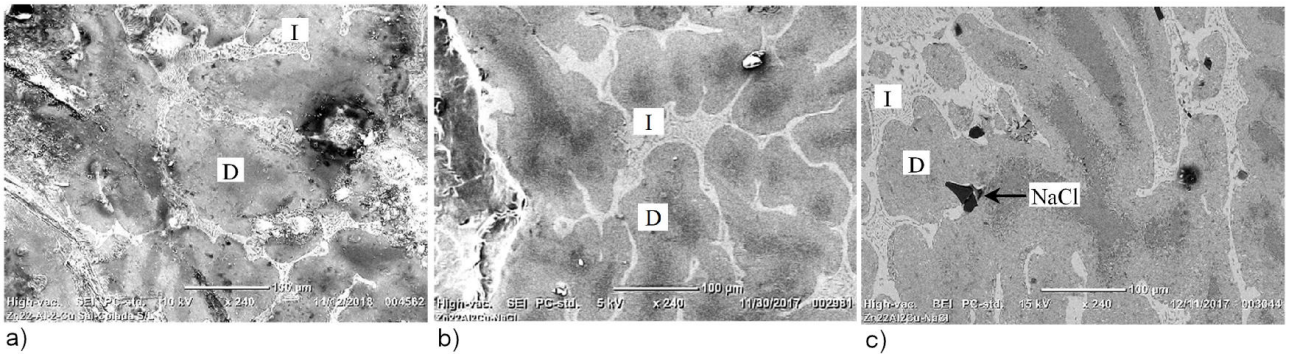

FIGURE 1. a) Initial cast-metal matrix microstructure and the resulting microstructures for b) 47.6% and c) 82% section reduced composites rolled at 230°C. D: dendrite, I: interdendritic zone.

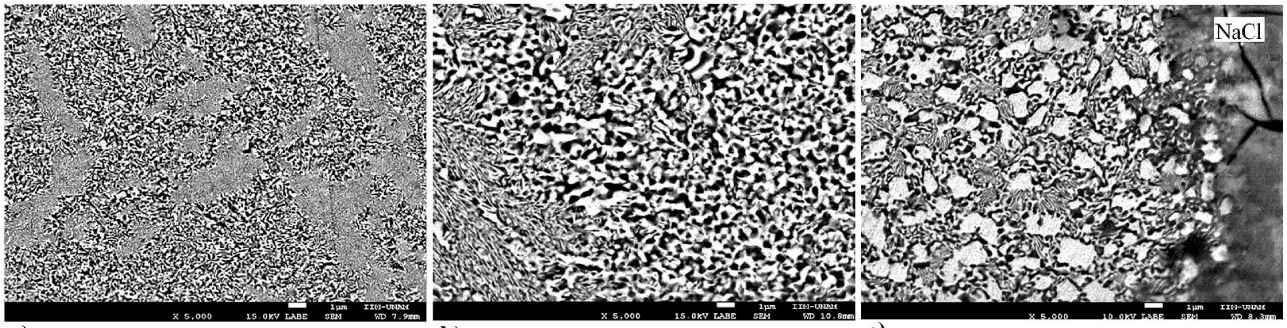

FIGURE 2. a) Initial fine-grained matrix microstructure and the resulting matrix microstructures for b) 58.33% and c) 78% section reduced composites hot-rolled at 230°C.

TABLE II. Composition of the nonrolled fine-grained matrix microstructure and constituents in the composite hot-rolled to 78% as measured by EDXS.

	Not rolled			78% **hot-rolled**		
Constituent or region	Zn(%p)	Al(%p)	Cu(%p)	Zn(%p)	Al(%p)	Cu(%p)
Dark embedded region [see Fig. 2c)]	*	*	*	63.91	34.24	1.85
Thin pearlite-type substructure (see Fig. 2c)]	*	*	*	70.82	27.26	1.92
Fine particles [see Fig. 2a)]	77	21	2	74.24	23.99	1.77
Light embedded islands [see Fig. 2c)]	*	*	*	84.70	12.20	3.10

The microstructure obtained in the matrix with the application of heat treatment is shown in Fig. 2a): the microstructure was composed of two types of alternating regions with fine constituents alternating between light (rich in Zn) and dark (rich in Al). One type of region had much finer constituents. This microstructure is hereafter called the fine-grained matrix microstructure.

The composition of the initial fine-grained matrix microstructure is shown on the left side of Table II, which was approximately the overall composition of the alloy matrix.

3.1.2. Microstructures produced by hot-rolling

The matrix microstructures of the initial cast-metal 47.6% and 82% hot-rolled composites are shown in Figs. 1b) and 1c), respectively. These figures show that the dendrites and interdendritic components became increasingly deformed as the rolling percentage increased.

The compositions established by EDXS in different zones (dendrite center, dendrite edge, interdendritic contour and interdendritic zone) of the microstructures obtained in the initial cast-metal 47.6% hot-rolled composite are presented on the right side of Table I.

These data show that the content of Zn goes from lowest to highest and that of Al from highest to lowest from the center of the dendrites to the interdendritic zone, as established in the initial cast-metal microstructure. The Cu content was null in the dendrite center and edge and was higher in the interdendritic contour than in the interdendritic zone. In addition, the contents of all the detected elements were higher in all the zones of this matrix microstructure compared with those established in each similar zone in the microstructure of the nonrolled cast-metal matrix composite.

Figure 3 shows micrographs at higher magnification of the microstructures obtained after 47.6% and 82% hot-rolling of the initial cast-metal matrix composite. The figures clearly show that an increase in the size of the components of the dendrite substructure occurred when the rolling percentage increased.

Figures 2b) and 2c) present the microstructures obtained after 58.33% and 78% hot-rolling at 230°C of the initial fine-grained matrix composite. The size of the constituents increased, and then, new light and dark islands were formed; the former were greater in quantity, evenly distributed, and surrounded by regions of fine pearlite and a fine-particle substructure, increasing with the section percentage reduction at 230°C of the initial fine-grained matrix composite.

The compositions of the dark islands, regions with a fine pearlite substructure, regions of fine particles and light islands in the microstructure of the 78% hot-rolled composite with the initial fine-grained matrix microstructure are shown on the right side of Table II. All the alloying elements were present in these constituents.

The regions with Zn contents from lowest to highest and Al contents from highest to lowest were in the following order: the dark islands, regions with a fine perlite substructure, fine-particle regions, and light islands. The Cu content was approximately the same (between 1.77% and 1.92% by weight) in the first three constituents and slightly higher (by more than 1%) in the light islands. The contents of Zn and Cu decreased slightly in the fine-grained regions with rolling.

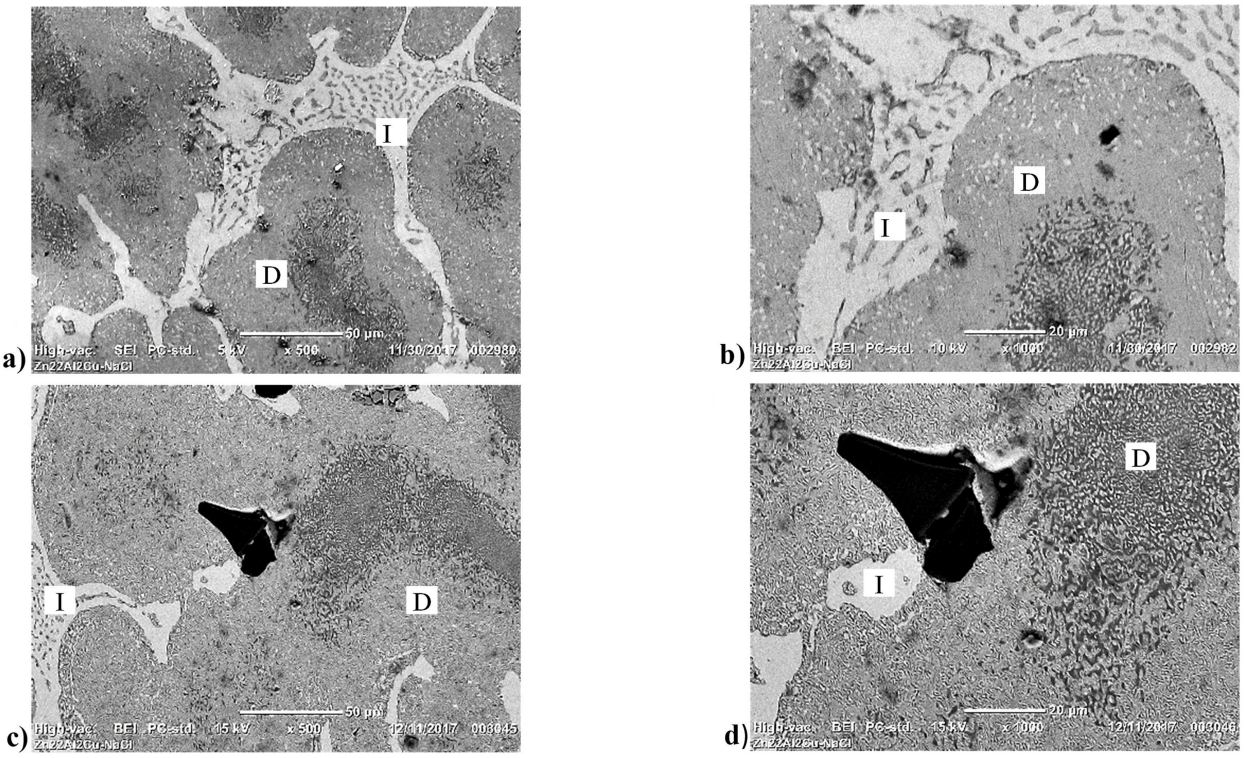

FIGURE 3. Higher magnification micrographs of the microstructures obtained for the initial cast-metal matrix composites with a) and b) 47.6% and c) and d) 82% section reduction at 230 . An increase in the size of the components of the dendrite substructure is observed when the % section reduction increases. D: dendrite, I: interdendritic zone.

3.2. Vickers microhardness and Rockwell hardness F

The variation of the Vickers microhardness at room temperature in the matrix and NaCl particles with section reduction of the composites with the two types of initial microstructures hot-rolled at 230 °C is shown in Fig. 4.

The initial fine-grained microstructure was harder than the initial cast-metal matrix microstructure, while the NaCl particles embedded in the fine-grained microstructure were softer than those in the cast-metal microstructure.

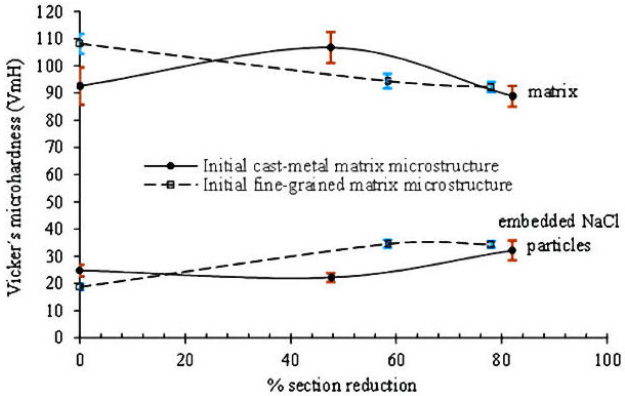

FIGURE 4. Variation of the Vickers microhardness established at room temperature in the matrix and NaCl particles with % section reduction of the initial cast-metal and fine-grained composites hot-rolled at 230°C.

For the initial fine-grained composite, the matrix was fully softened from the first stage of rolling and remained soft after the maximum section reduction; for the initial cast-metal composite, the matrix first hardened and then significantly softened with increasing section reduction.

In the fine-grained composite, the NaCl particles reached maximum hardness at the first stage of rolling, while for the cast-metal composite, the NaCl particles had almost constant hardness from the nonrolled state to the first stage of rolling and then acquired maximum hardness when the composite was hot-rolled to the maximum percentage.

The microhardness of the NaCl particles was considerably lower than the microhardness of the matrix for both types of microstructure before rolling and after each rolling step.

The variation of the Rockwell hardness F determined at room temperature in the two different composites with the section reduction at 230°C is shown in Fig. 5.

The hardness of the composites first increased and then substantially decreased with increasing section reduction regardless of the initial matrix microstructure, with the Rockwell hardness F being greater for the initial fine-grained composite.

4. Discussion

Images in Fig. 1 show that the components became increasingly elongated as the area reduction percentage of the com-

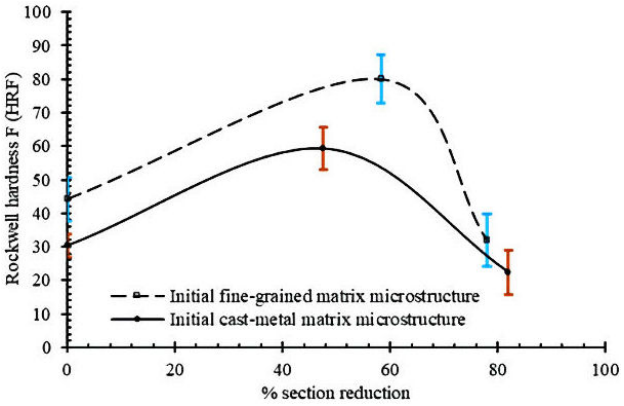

FIGURE 5. Variation of the Rockwell hardness F measured at room temperature with % section reduction of the initial cast-metal and fine-grained composites at 230°C.

posite increases. The cast-metal matrix microstructure then acquires the texture of the shape during the rolling process.

The initial fine-grained matrix microstructure undergo constituent growth and the formation of new phases and constituents, as seen in Fig. 2 and Table II; that is, this microstructure recrystallizes as hot rolling progresses.

The thermal energy and the energy contributed by rolling the initial cast-metal composite increased the Zn content of most of the components except the interdendritic region. These energies caused the compositions of the centers and edges of dendrites to become uniform, resembling the eutectoid Zn22Al composition reported in the Al-Zn equilibrium diagram [39]. The compositions of the interdendritic zone and the interdendritic contours approximated the eutectic Zn4.5Al composition, modified with Cu, of the same diagram. In addition, the Cu came out of the dendrites and entered the interdendritic zones and the interdendritic contours.

In the microstructure of the initial fine-grained composite rolled to a 78% section reduction at 230°C, the fine particle and fine pearlite regions had approximately the eutectoid compositions Zn22Al and Zn30.5Al, respectively, of the Al-Zn equilibrium diagram [39], but they had Cu. The light and dark islands were both rich in Zn and low in Cu content, but the dark islands had approximately 2.8 times as much Al as the light islands. The latter were nonequilibrium phases with compositions that did not resemble the phases reported in the aforementioned Al-Zn equilibrium diagram.

The lower microhardness of the NaCl particles in the initial fine-grained matrix was probably due to the increase of NaCl particle crystal size when the composite was maintained at 350°C for 45 hours before being tempered to produce the fine-grained microstructure in matrix.

The deformation of the constituents in the initial cast-metal composite caused hardening of the matrix to approximately 47.6% section reduction of the composite, while the increase in the size of the constituents and the appearance of new constituents due to increasing section reduction were associated with continuous softening of the initial fine-grained matrix, Fig. 4. Reportedly, the microstructure of fine particles softens when deformed [23,40].

The considerable softening of the matrix that occurred above the 47.6% section reduction of the composite with the initial cast-metal matrix microstructure could be due to the increase in the size of the constituents that form the dendrite substructure, as seen in Fig. 3.

The NaCl particles were hardened by deformation with increasing section reduction regardless of the matrix microstructure of the composite, hardening faster when the particles were embedded in the initial fine-grained microstructure, as seen in the lower part of Fig. 4.

Gabriel *et al.* reported [24] that the constituents of the fine-grained microstructure of the Zn22Al2Cu alloy are dislocation free. Thus, in the composite studied here with this matrix microstructure, the stress applied during rolling was transferred from constituent to constituent in the matrix and then almost entirely to the NaCl particles. For the initial cast-metal composite, the stress applied during rolling caused deformation of the cast-metal matrix, attenuating the stress ultimately applied to the particles embedded in the matrix. For this reason, hardening by deformation was achieved more quickly for the NaCl particles embedded in the initial fine-grained microstructure.

As seen in Fig. 5, the Rockwell hardness F variations established for both types of composites indicate that the NaCl particles oppose the plastic deformation of the matrix, acting as structural reinforcement until the first stage of section reduction. This effect becomes more evident when the microstructure transfers more stress to the NaCl particles, such as with the fine-grained microstructure, as explained in the previous paragraph.

This opposition of the NaCl particles to the plastic deformation of the matrix was more significant for the initial fine-grained microstructure. This is inferred because the Rockwell hardness F established of the fine-grained composite increased until the first stage of rolling, as seen in Fig. 5, although the matrix was continuously softened, the NaCl particles hardened slightly with rolling, and the particles were softer than the matrix, as seen in Fig. 4.

The decrease in the Rockwell hardness F of both types of composites from the first section reduction to the last section reduction, as seen in Fig. 5, maybe is due to the existence of more extensive areas of NaCl exposed on the surface of the plates, as seen in Figs. 7a) and 7b). Another factor causing this phenomenon could be the absence of a matrix below certain NaCl particles.

The Rockwell hardness F variation of the initial cast-metal matrix microstructure composite fully agreed with the microhardness variation of the matrix.

Figure 6 shows images of the initial cast-metal matrix microstructure composite for different percentages of section reduction. Through these images, deformation and thinning of the matrix and the embedded NaCl particles were observed as the percentage of section reduction increased.

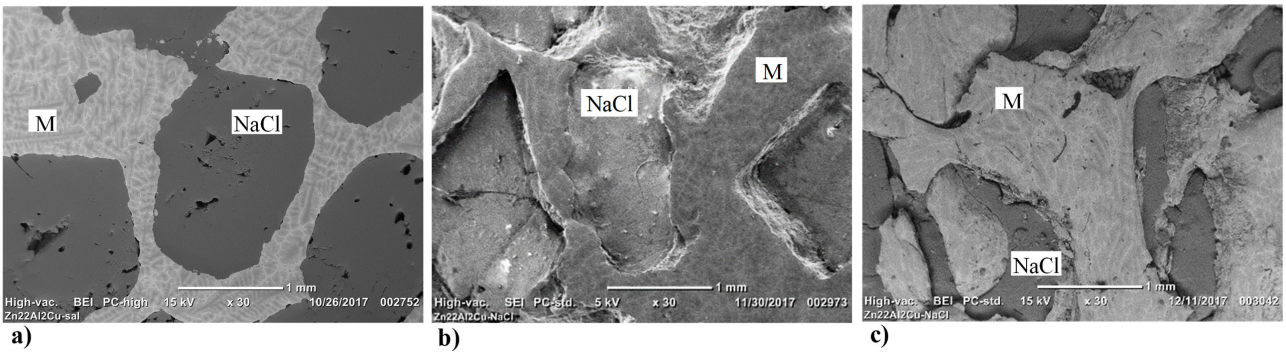

FIGURE 6. Micrographs of the initial cast-metal matrix microstructure composites a) not rolled and b) with 47.6% and c) 82% section reduction at 230°C. The increase in the deformation and thinning of the matrix and salt particles is observed with increasing section reduction. M: matrix.

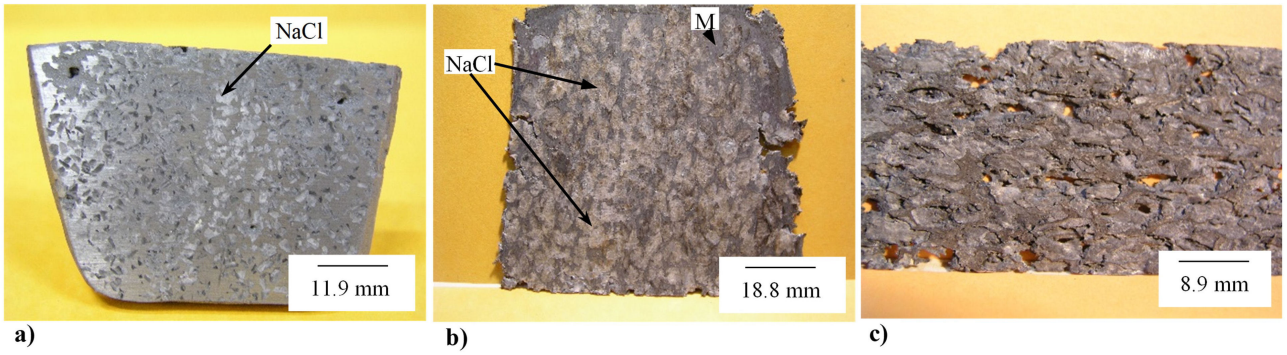

FIGURE 7. a) Nonrolled plate, b) sheet obtained with 82% section reduction of the Zn22Al2Cu-NaCl composite, and c) cellular sheet obtained by dissolving the NaCl in a sheet with 82% section reduction in boiling water. Initial cast-metal matrix microstructure. M: matrix.

The requirement of support of a greater percentage of stress imposed by the initial fine-grained microstructure on the NaCl particles results in increased brittleness in addition to the inherent brittleness of the salt, as NaCl is a solid formed by ionic bonds, which is associated with its hardening by deformation. This brittleness was evidenced by the presence of cracks in certain particles and by the separation or exfoliation of the NaCl particles of the composite hot-rolled at the maximum percentage when polishing or during ultrasonic cleaning of the samples, as seen on the right side of Fig. 2c).

Figure 7 shows a nonrolled plate, a piece of sheet of the initial cast-metal matrix microstructure composite with 82% section reduction, and a piece of sheet with the same initial microstructure and percent section reduction in which the NaCl was dissolved with boiling water, resulting in a cellular sheet of Zn22Al2Cu alloy.

A potential application of thin sheets of the Zn22Al2Cu-NaCl composite would be as an easily replaceable array of sheets in a receptacle that produces green hydrogen by splitting water molecules through alkaline hydrolysis: this method is considered one of the two main commercially available methods and is likely to become the dominant technology for green hydrogen production in the immediate future [41-44].

The metal in an array of sheets of this composite, forming a kind of cartridge, would be one of the electrodes immersed in the water to be hydrolyzed. After the NaCl dissolves in the water, the multiple cells of the Zn22Al2Cu cellular alloy would have a larger surface area, as shown in Fig. 7c), which could improve the efficiency of H_2 production in the receptacle. Once the salt has dissolved and the function of these sheets is completed, the cartridge can be removed and each of its sheets can be reused in one or more of the multiple recognized applications for cellular materials [34].

The very thin composite sheets, converted into cellular sheets, could also be used, for example, as air filters or heat sinks.

The proposed applications require complementary studies and measures to verify their viability.

5. Conclusions

Zn22Al2Cu-NaCl composite can be hot-rolled at 230°C. By increasing the section reduction of the composite, the constituents of the initial cast-metal matrix microstructure mainly acquire shape texture, the sizes of the dendritic substructures slightly increase, and the constituents tend to be similar in composition. In contrast, for the initial fine-grained microstructure, the constituents grow, and new constituents later appear. The NaCl particles are hardened by deformation with increasing section reduction of the composite, with the speed of hardening being greater when the matrix has an ini-

tial fine-grained microstructure. Hot-rolling to approximately 50% section reduction produces plates of Zn22Al2Cu-NaCl composite with increased hardness and plastic deformation strength when the initial matrix microstructure is fine-grained or cast. Thin sheets of cellular alloy Zn22Al2Cu can be obtained with this process under the conditions used in this work and by dissolving the salt in boiling water. Both microstructure types of this composite can be hot-rolled, with the cast-metal microstructure being more suitable because the integrity of the composite is maintained.

Acknowledgments

We thank Ing. Carlos Flores Moreno and Dr. Omar Novelo Peralta of the Institute of Materials Research of the Universidad Nacional Autónoma de México for their invaluable work in the operation of the scanning electron microscope.

1. W.A. Backofen, D.H. Avery and J.R. Turner, Superplasticity in Al-Zn alloy, *Trans. Am. Soc. Metals* **57** (1964) 980.
2. H.W. Hayden, R.G. Gibson and J.H. Brophy, Superplastic metals, *Sci. Amer.* **220** (1969) 28, https://www.jstor.org/stable/24926306
3. M. Demiras, G. Purcek, H. Yanar, Z.J. Zhang and Z.F. Zhang, Effect of different processes on lamellar-free ultrafine grain formation, room temperature superplasticity and fracture mode of Zn-22Al alloy, *J. Alloy. Compd.* **663** (2016) 75, https://doi.org/10.1016/j.jallcom.2015.12.142
4. S.H. Xia, J. Wang, J.T. Wang and J.Q. Liu, Improvement of room-temperature superplasticity in Zn-22 wt.%Al alloy, *Mater. Sci. Eng. A.* (2008) 111, https://doi.org/10.1016/j.msea.2007.07.100
5. K. Duong and F.A. Mohamed, Effect of impurity content on boundary sliding behavior in the superplastic Zn-22% Al alloy, *ActaMater* **46** (1998) 4571, https://doi.org/10.1016/S1359-6454(98)00128-1
6. B. Azad, A.R. Eivani and M.T. Salehi, Effect of Aging Process on Microstructure evolution and mechanical properties of UFG Zn-22Al alloy, *Iranian J. Mater. Sci. Engineering.* **20** (2023) 1, Doi:10.22068/ijmse.3278.
7. A. Yousefiani and F. A. Mohamed, Superplastic Flow and cavitation in Zn-22 Pct Al doped with Cu, *Metall. Mater. Trans. A* **29** (1998) 1653, https://doi.org/10.1007/s11661-998-0088-z
8. H. J. Dorantes-Rosales, V. M. López-Hirata, M. L. Saucedo-Muñoz, F. Hernández-Santiago, and R, Esquivel-González, Effect of prior cold working on microstructural evolution of precipitation in Zn22Al2Cu alloy during aging. *Mater. Sci. Tech.* **22** (2006) 1219, https://doi.org/10.1179/174328406X118230
9. P. C. Sharath, K. Rajendra Udupa, and G. V. Preetham Kumar, Effect of multi directional forging on the microstructure and mechanical properties of Zn-24 wt% Al-2 wt% Cu alloy, *Trans. Indian Inst. Met.* **70** (2017) 89, https://doi.org/10.1007/s12666-016-0863-2
10. M. Ramos *et al*., Phenomenological model for the dynamic superplastic deformation mechanism in a Zn-Al eutectoid alloy modified with 2 wt% Cu, *Met. Mater. Int.* **30** (2024) 3014, https://doi.org/10.1007/s12540-024-01696-8.
11. D. Yousefi *et al*., Microstructural evolution and mechanical properties of multi-directionally forged Sip/ZA22 composite, *Arch. Civ. Mech. Eng.* **20** (2020) 1, https://doi.org/10.1007/s43452-020-00124-z.
12. B. Azad, A. R. Eivani, and M. T. Salehi, Effect of Ti addition on microstructure and mechanical properties of Zn-22Al alloy after ECAP. *J. Cent. South Univ.* **31** (2024) 3703, https://doi.org/10.1007/s11771-024-5615-6.
13. S.R. Casolco, M. Lopes Parra, and G. Torres Villaseñor, High strain rate superplasticity of a Zn-22 wt.%Al-x wt.%Ag alloys, *J. Mater. Process. Tech.* **174** (2006) 389, https://doi.org/10.1016/j.matchar.2003.09.011
14. E. M. Ahmed, Physical properties of Zn-22 wt.% Al- x wt.% Ce melt spun eutectoid alloy, *Cryst. Res. Technol.* **47** (2012) 689, https://doi.org/10.1002/crat.20120009
15. P. K. Chahury, Kyung-Tae Park, and F. A. Mohamed, Effect of Fe on the superplastic deformation of Zn-22 pct Al, *Metall. Mater. Trans.* **25**A (1996) 2391, https://doi.org/10.1007/BF02648859
16. M. S. Gurjar, S. Dehiya1, M. Sharma, and N. C. Upadhyay, Effect of fly ash particles on the mechanical properties of Zn-22%Al alloy via stir casting method, *J. Mech. Civil. Eng.* **10** (2013), 39, https://www.iosrjournals.org/iosr-jmce/papers/vol10-issue2/G01023942.pdf
17. T. Jaglinski and R. S. Lakes, Zn-Al-based metal-matrix composites with high stiffness and high viscoelastic damping. *J. Compos. Mater.* **46** (2011) 755, https://doi.org/10.1177/0021998311410503
18. J. Wang *et al*, The apparent viscosity of fine particle reinforced composite melt, *J. Mater. Process. Tech.* **136** (2003) 60, https://doi.org/10.1016/S0924-0136(02)00919-6
19. A.H. Astaraie, H. R. Shahverdi, and S. H. Elahi, Compressive behavior of Zn-22Al closed-cell foams under uniaxial quasi-static loading, *Trans. Nonferrous Met. Soc. China* **25** (2015) 162, https://doi.org/10.1016/S1003-6326(15)63591-9
20. S. Ogawa, K. Sekido, and K. Kitazono, Energy absorption of superplastic Zn-22Al alloy foam manufactured through melt foaming process, *Mater. Sci. Forum.* **838-839** (2016) 231, https://doi.org/10.4028/www.scientific.net/MSF.838-839.231

21. A. Daoud, Synthesis and characterization of novel ZnAl22 syntactic foam composites via casting. *Mater. Sci. Eng. A.* **488** (2008) 281, https://doi.org/10.1016/j.msea.2007.11.020

22. J. Liu, S. Yu, X. Zhu, M. Wei, Y, Luo, and Y. Liu, Correlation between ceramic additions and compressive properties of Zn-22Al matrix composite foams, *J. Alloy Compd.* **476** (2009) 220, https://doi.org/10.1016/j.jallcom.2008.09.069

23. J. Negrete, A. Torres, and G. Torres-Villaseñor, Microstructural changes during hot rolling of Zn-Al eutectoid alloy with 2% Cu, *Mater. Manuf. Process.* **15** (2000) 199, https://doi.org/10.1080/10426910008912982

24. G. Torres, J. Negrete, and L. Valdés, Propiedades y usos del Zinalco, *Rev. Mex. Fis.* **31** (1985) 489.

25. M. Ramos, E. Martinez, and G. Torres, Superplastic behavior of Zn-Al eutectoid alloy with 2% Cu *J. Mater. Sci*. **47** (2012) 6206, https://doi.org/10.1007/s10853-012-6494-z

26. G. Torres-Villaseñor, and E. Martinez-Flores, Hibrid Materials based on Zn-Al alloys, in J. Cuppoletti, Ed., Metal, ceramic and polymeric composites for various uses (In-Tech, Florida, US, 2011) pp. 149-170, https://www.researchgate.net/publication/261835728_7_Hybrid_Materials_Based_on_Zn-Al_Alloys

27. J. A. Aragon and J. R. Miranda, Materiales compuestos de matriz metálica rica en Zn con alto contenido de Al y componente estructural de ZnO, *Rev. Mex. Fis.* **51** (2005) 356, ISSN 0035-001X

28. J. A. Aragon-Lezama, A. Garcia-Borquez and G. Torres-Villaseñor, Foam behavior of solid glass spheres - Zn22Al2Cu composites under compression stresses, *Mater. Sci. Eng. A.* **638** (2015) 165, https://doi.org/10.1016/j.msea.2015.04.048.

29. R. C. Flores-Marquez, J. A. Aragon-Lezama, and G. Torres Villaseñor, Effects of the size and matrix microstructure on compression of borosilicate spheres-Zn22Al2Cu composites with foam behaviour, *Rev. Mex. Fis. Rev*. **65** (2019) 31, ISSN 0035-001X.

30. W. Zhang, X. Ma, and D. Ding, Aging behavior and tensile response of a SiCw reinforced eutectoid zin-aluminium-copper alloy matrix composite, *Alloy. Compd.* **727** (2017) 375, https://doi.org/10.1016/j.jallcom.2017.08.130

31. A. Sanchez, A. Cruz, J. E. Rivera, J. A. Romero, M. A. Suárez, and V. H. Gutiérrez, Manufacturing of open-cell Zn-22Al-2Cu alloy foams by a centrifugal-replication process, *Metall. Mater. Trans.* **49**A (2018) 272, https://doi.org/10.1007/s11661-017-4390-5

32. S.R. Casolco *et al*., Processing and mechanical behavior of Zn-Al-Cu porous alloys, *Mater. Sci. Eng. A.* **471** (2007) 28, https://doi.org/10.1016/j.msea.2007.03.009

33. J. Banhart, Manufacturing routes for metallic foams. *Solidif. Sci., JOM* **52** (12) (2000) 22, https://doi.org/10.1007/s11837-000-0062-8

34. H.P. Degischer, B. Kriszt, Handbook of cellular metals: production, processing, applications, (Wiley-VCH, Hoboken, NJ, 2002), pp 179-183, ISBN: 3-527-30339-1. https://doi.org/10.1002/3527600558

35. J. A. Aragon-Lezama, A. Garcia-Borquez and G. Torres-Villaseñor, Assessment of NaCl grain texture and matrix microstructure on the room-temperature compressive behavior of Zn22Al2Cu-NaCl composite for future fabrication of cellular sheets via deformation (Its drafting is about to be finalized for future submission and publication.) (2026).

36. R. W. Davidge and P. L. Pratt, Plastic deformation and work-hardening in NaCl, *Physica Status Solidi (b)* **6** (1964) 759, https://doi.org/10.1002/pssb.19640060315

37. R. W. Davidge, Mechanical behavior of ceramics, Chpt 4 (Cambridge Univesity Press, NY, 1979), pp. 62, ISBN 13: 9780521219150

38. K. U. Kainer, Metal matrix composites. Custom-made Materials for Automotive and Aerospace Engineering (Wiley-VCH, 2006), https://doi.org/10.1002/3527608117

39. A. A. Presnyakov, Y. A. Gotban and V. V. Chervyakova, Aluminium-Zinc phase diagram, *Phys. Chem.* **55** (1961) 623.

40. J. L. Hernández-Rivera *et al*, Evaluation of hardening and softening behaviors in Zn-21Al-2Cu alloy processed by equal channel angular pressing, *J. Mater. Res. Technol.* **6** (2017) 329, https://dx.doi.org/10.1016/j.jmrt.2017.06.006

41. I. Dincer and C. Acar, Innovation in hydrogen production, *International Journal Hydrogen Energy* **42** (2017) 14846, https://doi.org/10.1016/j.ijhydene.2017.04.107

42. Alkaline Water Electrolysis Dominates with 55.3% Market Share in 2024, Anticipated to Grow at 60.3% CAGR by 2034, 2026-01-11, https://uk.finance.yahoo.com/news/alkaline-water-electrolysis-dominates-55-120200618.html.

43. Green Hydrogen Market Size, Share, and Growth Analysis, 2026-01-11, https://www.skyquestt.com/report/green-hydrogen-market.

44. Electrolyzer Market, 2026-01-11, https://www.fortunebusinessinsights.com/electrolyzer-market-103919